The LINNEAN SOCIETY of London ZOOLOGICAL Journal of the Linnean Society

Zoological Journal of the Linnean Society, 2016, **178**, 410–430. With 5 figures

Phylogeography and demographic history of the Andean degu, *Octodontomys gliroides* (Rodentia: Octodontidae)

DANIELA S. RIVERA[1,2]*, JULIANA A. VIANNA[3], LUIS A. EBENSPERGER[1] and R. EDUARDO PALMA[1]

[1]*Departamento de Ecología, Facultad de Ciencias Biológicas, Pontificia Universidad Católica de Chile, Casilla 114-D, Santiago, Chile*
[2]*Centro de Biodiversidad y Genética, Facultad de Ciencias y Tecnología, Universidad Mayor de San Simón, Cochabamba, Bolivia*
[3]*Departamento de Ecosistemas y Medio Ambiente, Facultad de Agronomía e Ingeniería Forestal, Pontificia Universidad Católica de Chile, Santiago, Chile*

Received 4 August 2015; revised 15 December 2015; accepted for publication 7 February 2016

The Andean degu, *Octodontomys gliroides* Gervais & d'Orbigny, 1844, has a broad distribution inhabiting pre-Andean pre-Puna and Puna environments of tropical South America. In order to understand the phylogeographic patterns of *Octodontomys gliroides*, we sequenced 579 bp of the mitochondrial DNA control region from 100 individuals collected from 20 populations across its entire distributional range. The phylogenetic and parsimony network, in conjunction with analysis of molecular variance (AMOVA), revealed a structured pattern of geographic differentiation of *O. gliroides*, with the occurrence of two well-defined evolutionary lineages: lineage A, restricted to Bolivia and Chile, and lineage B, restricted mainly to Argentina. Analysis of population structure inferred three genetic clusters along the distribution of *O. gliroides* that mostly agree with the four major barriers inferred by BARRIER analysis (e.g. rivers, salt flats, deserts, and mountain systems). In addition to the significant differentiation found among all levels studied, a positive correlation was identified between genetic and geographic distance, similar to as expected under the isolation-by-distance model. The most recent common ancestor of *O. gliroides* was estimated as *c.* 5.99 Mya, and the divergence between lineages A and B is estimated to have occurred by the Middle Pleistocene, about 0.69 Mya. The mismatch distributions and neutrality tests suggested a signal of population range expansion for both lineages coincident with major climatic changes that occurred during the wet–dry events of the Pleistocene in the Andean Puna region. Bayesian skyline plots (BSPs) for lineage A suggest a long history of constant population size followed by a period of slight to moderate demographic expansion at *c.* 0.04 Mya, whereas lineage B remained unclear after BSP analysis, probably because of the limited sample size.

© 2016 The Linnean Society of London, *Zoological Journal of the Linnean Society*, 2016, **178**: 410–430
doi: 10.1111/zoj.12412

ADDITIONAL KEYWORDS: Andes – climate – geography – Hystricognath – lineage – octodontids – population – Puna – rodents – social – South America.

Downloaded from https://academic.oup.com/zoolinnean/article/178/2/410/2674316 by guest on 10 January 2021

INTRODUCTION

The Octodontidae (degus, cururos, and viscacha rats) is an endemic family of Hystricognath rodents distributed along South America (Reig, 1981; Mares & Ojeda, 1982). This family represents one of the most characteristic groups in the arid lands of southern South America (Ojeda, 2010), ranging along both sides of the Andes in Argentina, Bolivia, and Chile, between 15 and 40°S (Ojeda *et al.*, 2013). Within this narrow geographical range, the Octodontidae occurs in a diverse array of habitats, including coastal areas in central Chile, pre-Andean and Andean regions, desert and semi-desert scrublands, and extremely arid salt flats (Contreras, Torres-Mura & Yánez,

*Corresponding author. E-mail: drivera@bio.puc.cl

1987; Gallardo *et al.*, 2007). In addition, these rodents include species that are ecologically, morphologically, and physiologically diverse, with cursorial, rock-dwelling, semi-subterranean, and truly subterranean forms (Contreras *et al.*, 1987; Lacey & Ebensperger, 2007). Interestingly, this diversity of characteristics seems to covary with patterns of social organization and behaviour (Ebensperger & Cofré, 2001; Lacey & Ebensperger, 2007), and where species range from being solitary to being highly social (Reig, 1986; Contreras *et al.*, 1987; Lacey & Ebensperger, 2007). Additionally, the octodontids are of great biogeographic and evolutionary interest because their origin and diversification reflect a dynamic scenario associated with environmental changes linked to the Andes uplift on both sides of the Andean Cordillera (Ojeda *et al.*, 2013).

Living Octodontidae are a monophyletic group that comprise 13 recognized species (Woods & Kilpatrick, 2005; Ojeda *et al.*, 2013) assigned to six monotypic and two polytypic genera (Ojeda *et al.*, 2013). Eight of the 13 species occur exclusively in Chile, ranging from coastal areas to the Andes: *Aconaemys fuscus* (Waterhouse, 1842), *Aconaemys porter* (Thomas, 1917), *Aconaemys sagei* (Pearson, 1984), *Octodon bridgesi* (Waterhouse, 1845), *Octodon degus* (Molina, 1782), *Octodon lunatus* (Osgood, 1943), *Octodon pacificus* (Hutterer, 1994), and *Spalacopus cyanus* (Molina, 1782). Four species inhabit extremely arid salt flats in Argentina: *Octomys mimax* (Thomas, 1920), *Pipanacoctomys aureus* (Mares *et al.*, 2000), *Salinoctomys loschalchalerosorum* (Mares *et al.*, 2000), and *Tympanoctomys barrerae* (Lawrence, 1941), and a single species (*Octodontomys gliroides* Gervais & d'Orbigny, 1844) simultaneously occupies the Andean region of northern Argentina and Chile and central–southern Bolivia (Contreras *et al.*, 1987; Ojeda *et al.*, 2013).

Most importantly, *O. gliroides* (the Andean degu) is the only octodontid rodent living in tropical South America, in environments with contrasting climatic and geographical characteristics, ranging from the north mesic Puna in Bolivia to the northern boundary of the Atacama Desert in Chile and north-western Argentina (Ojeda, Blendinger & Brandl, 2000; Woods & Kilpatrick, 2005). The current geographical distribution of *O. gliroides* matches a rainfall gradient from east to west created by the rain-shadow effect of the Andes. Although the Quaternary history of the rest of the octodontids has been punctuated by a pattern of glacial advances and retreats that resulted in extreme environmental changes from Andean Puna to Tierra del Fuego (Verzi & Quintana, 2005; Gallardo *et al.*, 2013), recent evidence suggests that the current distribution of *O. gliroides* could be associated with a complex history of dry–wet periods during the Pleistocene–Holocene in the central Andean Puna (Nester *et al.*, 2007; Placzek, Quade & Patchett, 2011). In particular, extensive flood cycles in the last 0.02 Myr produced large palaeolakes that divided the western and eastern sides of the Andean Puna (Placzek, Quade & Patchett, 2013), affecting the local climate of this region, which in turn affected the distribution of vegetation. How these changes in climate and connectivity in the Andean Puna have affected the current distribution of populations and phylogeographic history of *O. gliroides* has not been evaluated.

In recent years a single study has investigated the biology and ecology of *O. gliroides* (Rivera *et al.*, 2014). Andean degu are nocturnal, medium-sized species (~156 g) that feed mostly on ground-level cacti, columnar cacti, and shrubs (Rivera *et al.*, 2014). Andean degu are social rodents, where one or two females and one or two males share an underground burrow system (Rivera *et al.*, 2014); however, no studies have addressed the level of genetic differentiation among the Andean degu population.

We conducted this study to examine the genetic structure and phylogeographic patterns of *O. gliroides*, estimating the divergence time and assessing the demographic history of their populations. To achieve these goals, we sequenced the mitochondrial DNA (mtDNA) control region from specimens of this species across its entire distributional range. This information is critical to elucidate the historical and geographical context in which the evolution of *O. gliroides* took place.

MATERIAL AND METHODS

Study area and sample collections

Specimens and tissue samples were collected in the field from 11 localities across northern, central, and southern Bolivia, and from one locality in northern Chile. Skulls, skins, and tissues from Bolivian localities were deposited at the Colección Boliviana de Fauna, La Paz, Bolivia, and at the Museo de Historia Natural Alcides d'Orbigny, Cochabamba, Bolivia. Fieldwork for this study followed the American Society of Mammalogists guidelines for the handling of small mammals (Animal Care and Use Committee, 1998; Sikes & Gannon, 2011). Animal collection permits were granted by the Bolivian and Chilean authorities [permit number MMAyA-VMA-DGBAP N 0937/11, from the Dirección General de Biodiversidad y Areas Protegidas, Bolivia; authorization number 1-62-2012 (2373), from the Servicio Agrícola y Ganadero, Chile]. All procedures that involved the handling of live animals were approved by the Bioethical Committee of the Faculty of Biological

Downloaded from https://academic.oup.com/zoolinnean/article/178/2/410/2674316 by guest on 10 January 2021

Sciences at Pontificia Universidad Católica de Chile (CBB-040-2011).

To optimize the number of samples and to cover the full geographic range of the species, additional tissues and/or skin pieces were requested from collections and museums of Argentina (Museo Municipal de Ciencias Naturales 'Lorenzo Scaglia'; Colección de Mamíferos del Instituto Argentino de Investigaciones de zonas Áridas, IADIZA, and Catálogo de campo de Jorge Pablo Jayat), Chile (Colección de Flora y Fauna Profesor Patricio Sánchez Reyes, Pontificia Universidad Católica de Chile and Instituto de Ciencias Ambientales y Evolutivas, Universidad Austral de Chile), and the USA (Field Museum of Natural History, Chicago, Illinois, and the Sam Noble Oklahoma Museum of Natural History, The University of Oklahoma). All samples are listed and documented in Table 1.

DNA extraction, amplification, and sequencing

Genomic DNA extractions were performed using the phenol-chloroform method (Sambrook, Fritsch & Maniatis, 1989). An 800-bp fragment of the mtDNA control region (CR) was amplified by polymerase chain reaction (PCR) from 100 individuals using primers FVAL (5′-GAAAACAAACTCCTCAAATGAAG-3′) and H191 (5′-ATTATGCGGGCTAAGGGAACTG-3′), designed to amplify the same mtDNA region for related species of *O. gliroides*, *Tympanoctomys barrerae* (Ojeda, 2010), and *Octodon degus* (Valladares, 2009). Amplifications were performed using a thermal cycler (Applied Biosystems 2720) with the following parameters: initial denaturation at 94 °C for 3 min; 30 cycles of 45 s at 94 °C; 1 min at 50 °C; 1 min at 72 °C; and with a final extension for 5 min at 72 °C. All amplifications, including positive and negative controls, were checked in a 2% agarose gel with tris-acetic-acid buffer, using the proper molecular-weight ladder, and gels were visualized in an ultraviolet (UV) transilluminator. Double-stranded PCR products were purified with Wizard SV Gel and PCR Clean-Up System (Promega). All PCR products were sequenced by Macrogen Inc. (Seoul, South Korea; http://www.macrogen.com).

Phylogenetic analysis and divergence times

Phylogenetic relationships among mtDNA CR haplotypes of *O. gliroides* were inferred using Bayesian phylogenetic analysis performed in BEAST 1.7.4 (Drummond *et al.*, 2012). The best-fitting model of nucleotide substitution was selected using the Akaike information criterion (AIC), implemented in MODELGENERATOR 0.85 (Keane *et al.*, 2006). To estimate the mutation rate, an uncorrelated log-normal relaxed molecular clock model was used to allow rate variation among branches (Drummond *et al.*, 2006). This approach better accommodates clock-like data and produces smaller highest posterior densities, compared with alternative models (Drummond *et al.*, 2006). We employed a coalescent process with constant size prior for the branching rates. Because no fossils or reliable geological evidence were available to calibrate a local molecular clock for populations of *Octodontomys*, we followed Opazo's (2005) estimations that dated the divergence of *Octodontomys* and *Octodon* + *Spalacopus* + *Aconaemys* genera around 6.07 ± 1.3 Mya. We used a normal prior calibration with a mean of 6.07 and standard deviations of 0.68 Mya (Opazo, 2005). Analyses were run for 5×10^7 generations, with parameters logged every 100 000 generations following a pre burn-in of 4000 generations. Multiple runs were conducted to check for stationarity and independent runs converged on a similar result. The output from BEAST was examined in TRACER 1.5 (Rambaut & Drummond, 2009) with 10% burn-in and the tree results were summarized using TreeAnnotator 1.7 (included in the BEAST package), with the maximum clade credibility tree, posterior probability limit set to 0.5, and summarizing mean node heights. The tree was visualized using FIGTREE 1.3.1 (Rambaut, 2010). As an out-group, we used the mtDNA CR sequence from *Octodon degus*, the closest relative to *O. gliroides* (Woods & Kilpatrick, 2005), obtained from the GenBank (accession number GQ168717).

Phylogeographic and genetic structure analyses

Sequences were aligned using CodonCode ALIGNER 1.5.1 (CodonCode Corporation, Dedham, MA) and collapsed into haplotypes using the FaBox package (Villesen, 2007) (http://users-birc.au.dk/biopv/php/fabox/). Analyses were performed across 20 populations from Argentina, Bolivia, and Chile (Table 1). Analyses were also performed across two major ecogeographical regions: the Andean Puna and the Andean pre-Puna (Table 1). The subdivision into regions was based on differences in altitude. In particular, the Andean Puna included locations that ranged from 3400 to 4500 m a.s.l. (Cabrera, 1968; Cabrera & Willink, 1973; Aagesen *et al.*, 2009). Andean pre-Puna included locations with altitudes of 2000–3400 m a.s.l. (Cabrera & Willink, 1973; López & Beck, 2002; Aagesen *et al.*, 2009). Additionally, we followed Beck (1985), Cabrera (1968), and Davis *et al.* (1997) to subdivide the Andean Puna across a rainfall gradient from north to south and from east to west of the Andes. Thus, the northern Puna represented the moist Puna, and the central Puna and southern Puna represented the dry Puna (Table 1).

Downloaded from https://academic.oup.com/zoolinnean/article/178/2/410/2674316 by guest on 10 January 2021

Table 1. Description of sampling localities of *Octodontomys gliroides* specimens in Bolivia (Bo), Chile (Ch), and Argentina (Ar)

Map references	Locality	Latitude	Longitude	Ecogeographical regions	Id code/Source	N	Haplotypes	GENELAND clusters
Bolivia								
Bo1	Llacasa	16°40′S	68°01′W	Northern Puna	DSR	12	6,9,12,13	I
Bo2	Eucaliptus	17°35′S	67°33′W	Central Puna	DSR	17	5–9	I
Bo3	Jirira	19°50′S	67°37′W	Southern Puna	DSR	5	8	I
Bo4	Hara	19°46′S	67°34′W	Southern Puna	DSR	7	8	I
Bo5	Castilluma	19°56′S	68°15′W	Southern Puna	DSR	5	3	III
Bo6	Uyuni	20°26′S	66°45′W	Southern Puna	DSR	11	10, 20–23	III
Bo7	Oploca	21°19′S	65°57′W	pre-Puna	DSR	6	10,14,15	III
Bo8	Tupiza	21°25′S	65°43′W	pre-Puna	DSR	5	10	III
Bo9	Villa Abecia	20°59′S	65°14′W	pre-Puna	DSR	7	10,24–26	III
Bo10	Cieneguillas	21°19′S	65°02′W	pre-Puna	FMNH[1]	1	4	II
Bo11	Iscayachi	21°29′S	64°58′W	Central Puna	DSR	2	6,10	III
Chile								
Ch1	Putre–Murmutani	18°12′S	69°49′W	Central Puna	CAEVUACH[2]	3	3	III
Ch2	Putre–Chungará	18°22′S	69°33′W	Central Puna	CAEVUACH	2	3	III
Ch3	Camiña Chusmiza	18°13′S	69′15′W	pre-Puna	CAEVUACH	3	1,2	III
Ch4	Chusmiza	19°41′S	69°10′W	pre-Puna	SSUC[3]/DSR	7	1,2,3	III
Argentina								
Ar1	Pucara del Tilcara	23°35′S	65°24′W	pre-Puna	MMPMa[4]	2	16,17	II
Ar2	Susques	24°00′S	66°30′W	Southern Puna	OMNH[5]	1	11	II
Ar3	San Antonio los Cobres	24°16′S	66°30′W	Southern Puna	CMI–RAO[6]	2	19	II
Ar4	Santa Victoria	22°13′S	65°12′W	pre-Puna	JPJ[7]	1	10	III
Ar5	Cachi	25°01′S	66°14′W	pre-Puna	OMNH	1	18	II

Localities and habitat type are shown in Fig. 2A. For all specimens we reported the ID code/museum or collection source and number of specimens (*N*) sampled in each population.
[1]Field Museum of Natural History, Chicago, Illinois, USA.
[2]Instituto de Ciencias Ambientales y Evolutivas, Universidad Austral de Chile, Valdivia, Chile.
[3]Colección de Flora y Fauna Profesor Patricio Sánchez Reyes, P. Universidad Católica de Chile, Santiago, Chile.
[4]Museo de Ciencias Naturales y Tradicional de Mar del Plata 'Lorenzo Scaglia', Mar del Plata, Argentina.
[5]Sam Noble Oklahoma Museum of Natural History, The University of Oklahoma, Norman, Oklahoma, USA.
[6]Colección de Mamíferos del Instituto Argentino de Investigaciones de zonas Áridas (IADIZA), Mendoza, Argentina.
[7]Catálogo de campo de Jorge Pablo Jayat, Tucumán, Argentina.

Genetic diversity within populations was estimated as numbers of haplotypes (*H*), haplotype diversity (*Hd*), nucleotide diversity (π), and the number of polymorphic sites (*PS*), using ARLEQUIN 3.5.1.2 (Excoffier & Lischer, 2010). These analyses were performed for each population, each ecogeographical region, and globally (considering all populations).

To infer the historical processes that shaped the sample populations, the relationships between haplotypes and geography were examined in a haplotype network. The network was constructed using TCS 1.21 (Clement, Posada & Crandall, 2000), which uses a 95% confidence limit for connecting haplotypes.

Spatially explicit information on population structure was analysed with a Bayesian approach implemented using GENELAND 4.0.3 (Guillot *et al.*, 2005a; Guillot, Mortier & Estoup, 2005b), which estimates the number of genetic clusters present in the data set and incorporates the geographical coordinates of the individuals to detect and locate genetic discontinuities (Guillot *et al.*, 2005a). Although there are other spatially explicit methods, such as SAMOVA (Dupanloup, Schneider & Excoffier, 2002), the application in GENELAND included the assessment of finer-scale patterns of population structure with a very low level of uncertainty in estimating the number of populations. Additionally,

Downloaded from https://academic.oup.com/zoolinnean/article/178/2/410/2674316 by guest on 10 January 2021

we followed Guillot *et al.*'s (2012: 898) in deciding to use GENELAND with non-recombining mtDNA sequences. The number of clusters was determined by running Markov chain Monte Carlo (MCMC) iterations five times, allowing K (i.e. the most probable number of populations) to vary, with the following parameters: 5×10^6 MCMC iterations and with the maximum rate of the Poisson process fixed to 100 (equal to the sample size, as recommended by Guillot *et al.*, 2005a). The minimum and maximum K values were fixed to 1 and 10, respectively. The maximum number of nuclei in the Poisson–Voronoi tessellation was fixed to 300 (roughly three times the sample size, as suggested by Guillot *et al.*, 2005a). After inferring the number of populations in the data set from these five runs, the MCMC was run 30 times with K fixed to the inferred number of clusters, while keeping all other parameters set as in the previous analysis. We ranked the models by mean logarithm of posterior probability and conducted post-processing analyses for the three runs with the highest values. We used a burn-in period of 1000×100 iterations, a spatial domain of 400 pixels along the x-axis and 200 pixels along the y-axis, and checked the runs visually for consistency.

The fixation index between two populations (pairwise F_{ST} values) and their linear geographical distances (in km) were used to examine patterns of isolation by distance (IBD). A Mantel test (Mantel, 1967) was used to assess the significance of the correlation between gene-flow estimates and geographical distances using 5000 permutations, as implemented in PAST 3.06 (Hammer, Harper & Ryan, 2001). We expected that populations separated by longer geographic distances would show higher genetic differences. As an overall assessment of geographic structure affecting population differentiation, a comparison of the two estimates of genetic variation, G_{ST} (based solely on differences in haplotype frequencies; Pons & Petit, 1995) and N_{ST} (based on differences in haplotype frequencies and the genetic distances between haplotypes; Pons & Petit, 1996), was performed with DnaSP 5.0 (Librado & Rozas, 2009). Therefore, when more closely related haplotypes are found in the same area than less closely related haplotypes, N_{ST} is significantly larger than G_{ST}, indicating a phylogeographic structure (Pons & Petit, 1996). Because some our samples came from localities in which only one or a few individuals were sampled, we pooled the Bo10 and Bo11 samples, the Ch1 and Ch2 samples, the Ch3 and Ch4 samples, the Ar1 and Ar4 samples, and the Ar2, Ar3, and Ar5 samples. This resulted in 14 populations, and the N_{ST} versus G_{ST} test was performed among this group of populations.

To provide a geographic representation of genetic discontinuities between populations, we identified the geographic areas associated with a genetic change using the method of Manni, Guérard & Heyer (2004), implemented in BARRIER 2.2. First, a Delaunay triangulation network was created to connect adjacent populations. A set of Voronoi polygons was derived from the corresponding Delaunay network. Each edge of the Voronoi tessellation was associated with the estimated value of the genetic distance between the two populations. Monmonier's maximum-difference algorithm was then applied to identify boundaries, starting from the edge for which the distance value was highest, and proceeding across adjacent edges until the boundary reached either the limits of the triangulation or another pre-existing boundary. The number of barriers needs to be defined *a priori*. We represented only barriers including values of pairwise genetic differentiation higher than the average calculated on the whole samples. Samples from some of the 20 populations were pooled for this analysis, as the distance estimates derived from 'populations' with very small sample sizes of only one or two samples were likely to be a poor estimate of the true values. Again we pooled the Bo10 and Bo11 samples, the Ch1 and Ch2 samples, the Ch3 and Ch4 samples, the Ar1 and Ar4 samples, and the Ar2, Ar3, and Ar5 samples, resulting in 14 populations. The genetic distances used in the BARRIER analysis were population pairwise F_{ST} values derived in ARLEQUIN 3.5.1.2 (Excoffier & Lischer, 2010).

To partition the total genetic variance into its hierarchical components among groups, among populations within groups, and within populations, we performed AMOVA using ARLEQUIN 3.5.1.2 (Excoffier & Lischer, 2010). For this analysis, geographic groups of populations were defined according to phylogenetic and network data, by GENELAND clusters, and by groups of populations according to the genetic boundaries identified by the Monmonier's maximum-differences algorithm. Significance values were derived using 100 000 permutations.

Finally, signatures of population demographic changes (bottlenecks or expansions) in *O. gliroides* were first examined by Tajima's D (Tajima, 1989) and Fu's F_S (Fu, 1997) neutrality statistics using ARLEQUIN 3.5.1.2 (Excoffier & Lischer, 2010). These neutrality tests assume that the population has been in mutation–drift balance for a long period of evolutionary time (Nei & Kumar, 2000). When the population is not under mutation–drift equilibrium, as a result of a sudden expansion in population size, these indexes tend to exhibit significantly negative values and an excess of polymorphisms at low frequency. By contrast, positive values reflect the

Downloaded from https://academic.oup.com/zoolinnean/article/178/2/410/2674316 by guest on 10 January 2021

elimination of rare alleles after genetic bottlenecks or processes such as a population subdivision (Ramos-Onsins & Rozas, 2002). Second, to evaluate the evolutionary history of lineages within *Octodontomys gliroides*, a sudden demographic history of expansion model (Rogers & Harpending, 1992) was tested by calculating the Harpending's raggedness index (r_H; Harpending, 1994) of the observed mismatch distribution for each of the populations according to the population expansion model implemented in ARLEQUIN 3.5.1.2 (Excoffier & Lischer, 2010). This measure quantifies the smoothness of the observed mismatch distribution. Small raggedness values represent populations that have experienced sudden expansion (i.e. unimodal distribution), whereas higher values of the raggedness index suggest stationary or bottlenecked populations (i.e. multimodal distribution; Harpending, 1994). Third, the demographic history of whether *O. gliroides* underwent a range expansion was investigated by the spatial expansion model in ARLEQUIN 3.5.1.2 (Excoffier & Lischer, 2010). Calculations were performed using 1000 permutations to test the goodness-of-fit of the observed mismatch distribution with that expected under the spatial expansion model using the sum of squared deviations (SSD). A significant SSD value was taken as evidence of a departure from the estimated demographic model of spatial expansion in subdivided populations (Excoffier, 2004). The expansion parameters theta initial (θ) and tau (τ) were calculated by the analysis.

Although D, F_S, and mismatch distributions provide insights into whether or not population growth has been expansive, they are not able to provide information about the shape of population growth over time. For example, non-significant negative values of D and F_S should indicate that populations have not undergone expansive growth (i.e. population stability); however, such values cannot indicate whether populations are expanding slowly, are contracting, or are remaining at relatively constant size (Fontanella *et al.*, 2008). Therefore, to estimate the shape of population growth through time we constructed a Bayesian skyline plot (BSP) as implemented in BEAST 1.7.4 (Drummond *et al.*, 2012). This Bayesian approach incorporates uncertainty in genealogy by using MCMC integration under a coalescent model, providing information about effective population sizes (N_e) through time (Drummond *et al.*, 2005). The best-fitting substitution model was estimated in MODELGENERATOR 0.85 (Keane *et al.*, 2006). The running conditions included 5.0×10^7 iterations, and where model parameters were sampled every 1000 steps under a relaxed lognormal molecular clock, with a fixed rate of calibration, and assuming a substitution rate of 10% per site per Myr (Brown, 1986). The first 10% of steps were discarded to allow for burn-in. To assess the robustness of parameter estimates, two independent chains were run with identical settings. Log files were visualized using TRACER 1.5 (Rambaut & Drummond, 2009). A slope in a skyline plot that does not significantly differ from zero would indicate that the population size has been constant through time. Mismatch distributions and BSP were built globally, and for each geographical group identified by phylogenetic and haplotype network analysis.

RESULTS

Phylogenetic analysis and divergence time

The best-fitting model of nucleotide substitution, as determined by MODELGENERATOR, was the Hasegawa, Kishino, Yano model plus invariable sites and gamma distribution (HKY+I+G), with $I = 0.43$ and $G = 0.06$. The Bayesian analysis recovered *O. gliroides* as a well-supported monophyletic group composed of two principal lineages, namely lineages A and B. Lineage A was widespread in Bolivia and Chile, and comprised 20 haplotypes in 93 individuals from populations in northern, central, and southern Bolivia, and northern Chile. Lineage B was geographically restricted mainly to Argentina, including six haplotypes in six individuals and one haplotype in a single individual belonging to the southern Bolivian population (H4; Fig. 1A). Lineage A can be further substructured into two sublineages: A1, comprising haplotypes from northern Chile, and central and southern Bolivia; and A2, including haplotypes from northern and central Bolivia. The two main lineages, A and B, were supported by high posterior probability values (Fig. 1A).

The divergence time analysis indicated that *Octodon degus* split from the ancestor of a form that gave rise to *Octodontomys gliroides* during the Late Miocene, *c.* 5.99 Mya (95% CI 4.69–7.33 Mya; Fig. 1A). The divergence time between lineage A and lineage B was estimated to have occurred during the Middle Pleistocene, *c.* 0.69 Mya (95% CI 0.14–1.58 Mya), whereas the divergence time between sublineages A1 and A2 was estimated to have occurred more recently, *c.* 0.35 Mya (95% CI 0.07–0.70 Mya; Fig. 1A).

Population Genetic Analysis

The sequence alignment of the mtDNA CR for *Octodontomys gliroides* showed a total of 24 variable sites, including four singletons and 20 parsimony-informative sites, defining 26 haplotypes (GenBank accession numbers: KF917586–KF917611; for the

Downloaded from https://academic.oup.com/zoolinnean/article/178/2/410/2674316 by guest on 10 January 2021

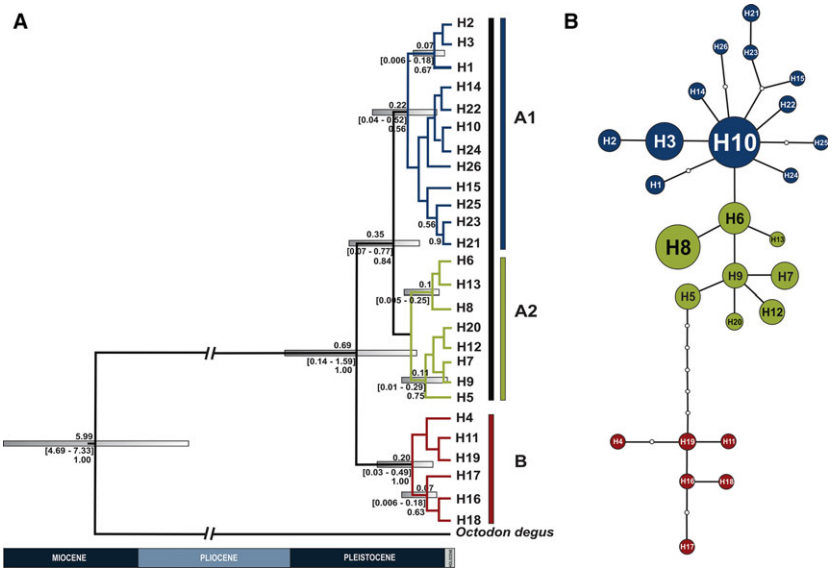

Figure 1. A, phylogenetic relationships within the principal nodes for *Octodontomys gliroides*, based on Bayesian analysis of mtDNA control region haplotypes. Divergence dates of the most recent common ancestor in million years (above the branches), 95% credible intervals (below the branches), and nodes with high posterior probability (below the 95% credible intervals) are shown. The two main lineages are indicated by black and red lines, and the sublineages found in lineage A, referred to in the text as A1 and A2, respectively, are coloured as follow: sublineage A1, blue; sublineage A2, green. B, haplotype network recovered by statistical parsimony analysis. Each circle represents a different haplotype with size proportional to frequencies, with the largest circles representing the most abundant haplotypes. The coloration pattern of each haplotype represents the lineages and sublineages recovered in the phylogenetic analysis. White circles denote the number of mutational steps between haplotypes. For geographical details of sampling populations and haplotype codes, see Table 1.

distribution of each haplotype among sampling localities, see Appendix 1 and Fig. 2A). The mtDNA CR sequences of *Octodontomys gliroides* showed a pattern of high haplotype diversity (*Hd* = 0.921 ± 0.01), but moderate nucleotide diversity (π = 0.0059 ± 0.0034; Table 2). At the population level, Bolivian populations (Bo10 and Bo11) and Argentine populations (Ar1, Ar2, Ar4, and Ar5) presented the highest values of haplotype diversity. The highest values of nucleotide diversity were found in populations Bo6, Chi3, and Ar1 (Table 2). Six populations, Bo3, Bo5, Bo8, Ch1, Ch2, and Ar3, were invariant. Of the remaining populations, the lowest value of haplotype diversity was found in Bo4 and the lowest value for nucleotide diversity was found in B11 (Table 2). At the ecogeographic regions, the Andean Puna presented the highest value of haplotype diversity and the lowest value of nucleotide diversity. Among the subdivisions at the Andean Puna, the haplotype diversity ranged from 0.77 for the northern Puna to 0.83 for the central Puna, whereas nucleotide diversity ranged from 0.0020 in northern Puna to 0.0058 in southern Puna (Table 2).

The parsimony network based on these 26 mtDNA haplotypes recovered two well-differentiated main haplotype groups, separated by seven mutational steps (Fig. 1B). One group connected all haplotypes found in northern Chile, and central and southern Bolivian populations, which corresponds with lineage A yielded by the phylogenetic analysis. This haplotype group also showed the subdivision corresponding to the sublineage A1 and A2, but only differentiated by one mutational step. The second group fully corresponded to the lineage B identified by phylogenetic analysis. The haplotype group corresponding to sublineage A1 and A2 showed a star-like structure centred on haplotype H10 (which was also the most frequent haplotype of the parsimony network) and H9, respectively. A star-like shape was less apparent for the haplotype group corresponding to lineage B, and was centred on haplotype H19 (Fig. 1B). Most of the 26 haplotypes were restricted to a single population and ecogeographic region (73% private haplotypes). Seven haplotypes (H1, H2, H3, H6, H8, H9, and H10) were shared among two or more populations, but only five haplotypes were shared among two or three ecoregions (Appendix 2). The most widely distributed haplotypes in the entire sample were H3, H8, and H10. H1 and H2 were found in three and five individuals, respectively,

Downloaded from https://academic.oup.com/zoolinnean/article/178/2/410/2674316 by guest on 10 January 2021

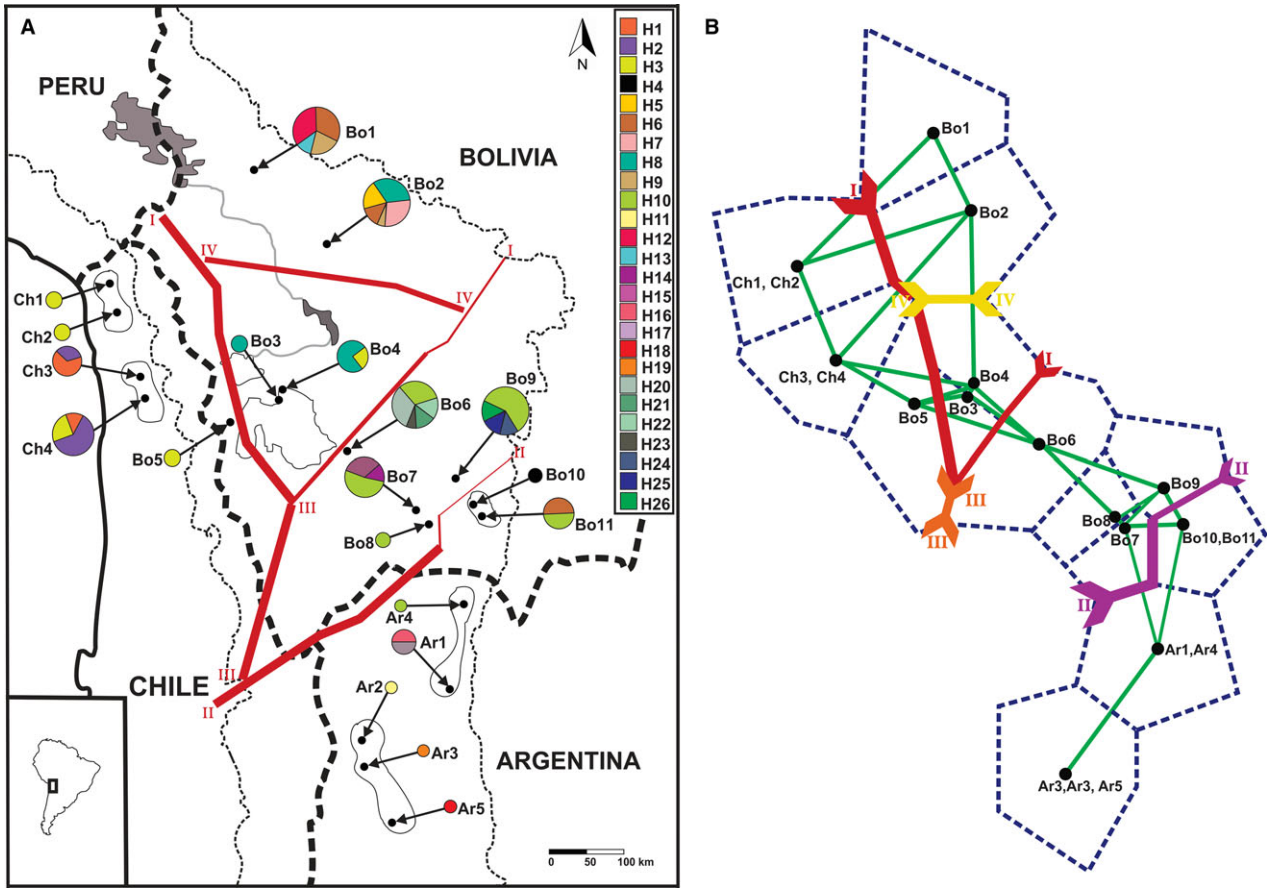

Figure 2. A, geographical location of the sampled populations along its distributional range (for abbreviations of localities, see Table 1), and results of the BARRIER analysis. Pie charts display the frequency of occurrence of each haplotype in each locality; the size of the pie chart is proportional to population size. The genetic barriers in red are numbered (in Roman numerals) and the thickness is proportional to the ratio between genetic distance values between populations on both sides of each barrier to the average genetic distance among populations in the whole data set. The populations inside unfilled irregular shapes are the populations pooled by the BARRIER analysis (for more detail, see Material and methods). B, the four major genetic boundaries (thick colored lines) detected by BARRIER 2.2 using F_{ST} values. The order of the numerical pairs represents the sequence of the boundary formation. The black dots correspond to the population numbers plotted along the ordination (some populations were pooled by the analysis). The dashed lines and solid lines represent the Voronoi tessellation and the Delaunay triangulation, respectively.

from Ch3 and Ch4 belonging to the Andean pre-Puna of Chile. H3 was found in 14 individuals restricted to five populations (Bo4, Bo5, Ch1, Ch2, and Ch4) belonging to the Andean Puna of Bolivia and Chile (central and southern Puna), and the Andean pre-Puna of Chile (see Appendix 2). H6 was found in seven individuals restricted to B1, B2, and B11 that belonged to the northern and central Puna of Bolivia. H8 was found in 15 individuals and in three populations (Bo2, Bo3, and Bo4) restricted to the Andean Puna occurring in both central and southern Puna. H10 was represented in 17 individuals from six populations (Bo6, Bo7, Bo8, Bo9, Bo11, and Ar4), restricted to the Andean pre-Puna and to a low proportion to the Andean Puna (central and southern Puna; see Appendix 2).

The population structure of *Octodontomys gliroides* estimated through GENELAND generated three genetic clusters (k = 3), designated I, II, and III (Fig. 3A; Table 1). Each population had a probability of 0.90–1.00 belonging to one of the assumed clusters (white area surrounded by the 0.90 isocline; Fig. 3B–D), providing strong support to the GENELAND results. Cluster I comprised all samples from the northernmost population of Bolivia (Bo1) and three populations from central Bolivia (Bo2, Bo3, and Bo4; Fig. 3B; Table 1). Cluster II was represented by all populations of northern Chile (Ch1–Ch4), central

Downloaded from https://academic.oup.com/zoolinnean/article/178/2/410/2674316 by guest on 10 January 2021

Table 2. Number of sequences, haplotypes, polymorphic sites by population, haplotype diversity *Hd* and nucleotide diversity (π), based on the mitochondrial DNA control region sequence

Sample locality	Number of sequences	Haplotype	Polymorphic sites	*Hd*	Standard deviation	π	Standard deviation
Bolivia							
Bo1	12	4	3	0.77	0.07	0.002	0.0016
Bo2	17	5	4	0.8	0.05	0.0031	0.0021
Bo3	5	1	0	0	0	0	0
Bo4	7	2	3	0.47	0.17	0.0025	0.0019
Bo5	5	1	0	0	0	0	0
Bo6	11	5	7	0.85	0.07	0.0049	0.0031
Bo7	6	3	3	0.73	0.15	0.0021	0.0017
Bo8	5	1	0	0	0	0	0
Bo9	7	4	6	0.71	0.18	0.0029	0.0022
Bo10	1	1	0	1	0	0	0
Bo11	2	2	1	1	0.5	0.0017	0.0024
Chile							
Ch1	3	1	0	0	0	0	0
Ch2	2	1	0	0	0	0	0
Ch3	3	2	3	0.67	0.31	0.0034	0.0033
Ch4	7	3	3	0.67	0.16	0.0019	0.0016
Argentina							
Ar1	2	2	2	1	0.05	0.0034	0.0042
Ar2	1	1	0	1	0	0	0
Ar3	2	1	0	0	0	0	0
Ar4	1	1	0	1	0	0	0
Ar5	1	1	0	1	0	0	0
Ecogeographical regions							
Andean Puna	67	15	16	0.89	0.02	0.0049	0.0029
Northern Puna	12	4	3	0.77	0.07	0.002	0.0016
Central Puna	19	6	5	0.83	0.04	0.0031	0.0021
Southern Puna	36	9	14	0.81	0.04	0.0058	0.0034
Andean pre–Puna	33	13	21	0.82	0.06	0.0066	0.0038
Total	100	26	24	0.92	0.01	0.0059	0.0034

The abbreviations of localities are as defined in Table 1.

and southern Bolivia (Bo5, Bo6, Bo7, Bo8, Bo9, and Bo11), and the northernmost population of Argentina (Ar4; Fig. 3C; Table 1). Cluster III comprised four of the southernmost populations from Argentina (Ar1, Ar2, Ar3, and Ar5) and one population from southern Bolivia (Bo10; Fig. 3D; Table 1).

The Mantel test revealed a significant positive correlation between genetic distances and linear geographical distances among populations ($r = 0.479$, $P < 0.05$). A comparison of N_{ST} and G_{ST} revealed a population differentiation within the entire range, with N_{ST} greater than G_{ST} (0.535 and 0.338, respectively), suggesting that there was a phylogeographic structuring of haplotypes. The overall differentiation among populations was very high ($F_{ST} = 0.535$). This suggests that closely related haplotypes in *Octodontomys gliroides* populations were found more often in the same area than less closely related haplotypes.

Geographic boundaries detected by BARRIER 2.2 are given in Fig. 2A, B. Monmonier's maximum-difference algorithm identified four putative barriers. The first barrier separated samples located in northern and central Bolivia (Bo1–Bo4) from all other samples. The second barrier separated central Bolivian samples (Bo6, Bo7, Bo8, and Bo9) from those located in southern Bolivia (Bo10 and Bo11), as well as all Argentinian samples. The third barrier separated all Chilean samples and Bo5 from samples located in central Bolivia (Bo6–Bo11). Finally, the fourth barrier separated the northernmost samples of Bolivia (Bo1 and Bo2) from Bo3 and Bo4.

The AMOVA identified significant values for the genetic variance at the three levels tested (among the lineages determined by phylogenetic and parsimony network analyses, among clusters defined by GENELAND, and among groups separated by the

Downloaded from https://academic.oup.com/zoolinnean/article/178/2/410/2674316 by guest on 10 January 2021

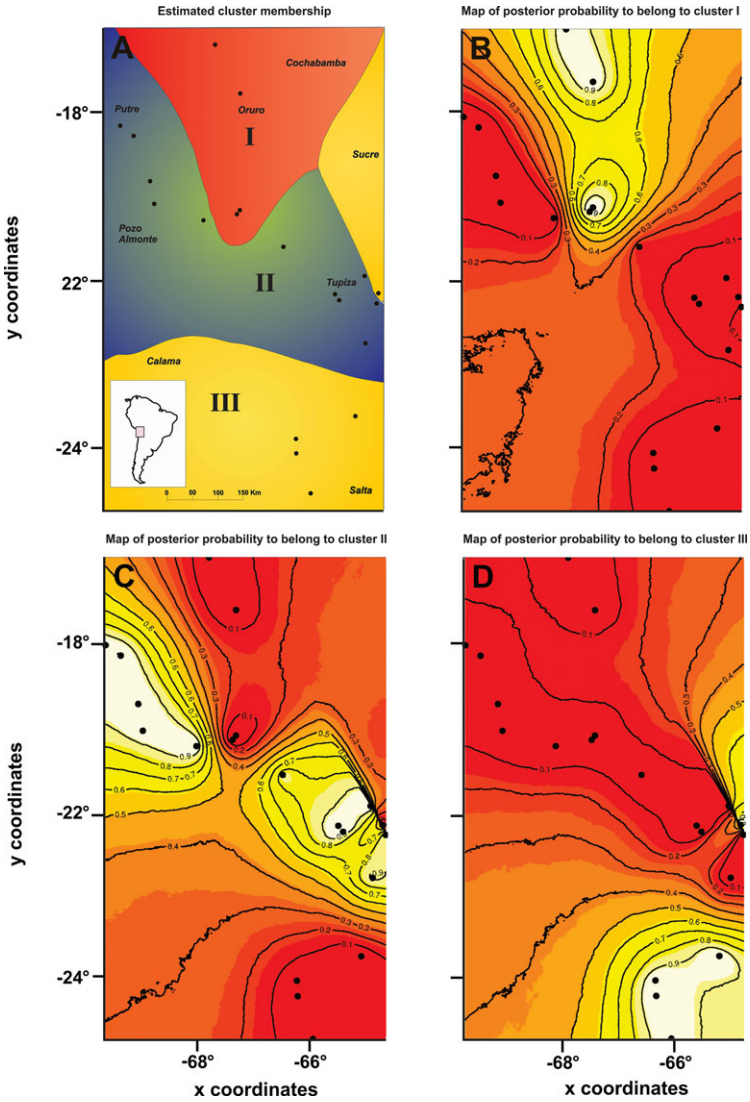

Figure 3. Map of cluster membership and posterior probability for each cluster based on the GENELAND analysis. A, the estimated cluster membership represents the modal cluster assignment of each pixel, and the rest of the inset maps show the posterior probability of individuals of *Octodontomys gliroides* in Argentina, Bolivia, and Chile. Black dots represent sampling localities. The three clusters are: B, populations of northern and central Bolivia; C, populations from northern Chile, central and southern Bolivia, and northern Argentina; and D, the remaining Argentinian populations and one population from southern Bolivia. The white area represents a probability between 90 and 100% for sampling localities to belong to their respective cluster.

most supported geographic breaks identified by the BARRIERS analysis; Table 3). Grouping populations by phylogenetic lineage explained more of the genetic variation (73.38%, $P < 0.001$; Table 3) than grouping populations by GENELAND clusters and BARRIER-based analysis (50.04%, $P < 0.001$, and 48.76%, $P < 0.001$, respectively; Table 3).

All demographic analyses found a consistent signature of population expansion in the recent past. The analysis showed negative and statistically significant values of Fu's F_S neutrality test at the global level ($F_S = -10.975$, $P = 0.001$) and for populations grouped by geographic regions (lineage A and lineage B; Table 4), suggesting a demographic range expansion process. In contrast, the Tajima's D-test did not reveal a signal of demographic expansion at the global scale ($D = -0.786$, $P = 0.193$). Similarly, signals of population expansion were not detected in any of the populations grouped by geographic regions (lineage A and lineage B; Table 4) using Tajima's D-test. The discrepancy between the D and F_S tests is likely to arise from the decreased statistical power of D in detecting

Downloaded from https://academic.oup.com/zoolinnean/article/178/2/410/2674316 by guest on 10 January 2021

Table 3. Analytic summary of analysis of molecular variance (AMOVA) based on pairwise differences of mitochondrial DNA control region for *Octodontomys gliroides*

Group level	Source of variation	d.f.	Sum of squares	Variance components	Percentage of variation (%)	Fixation index ($P < 0.005$)
Phylogenetic lineages	Among lineages A and B	1	48.026	3.539	73.38	$\Phi_{CT} = 0.734$
	Among sampled localities within lineages	18	66.34	0.605	12.55	$\Phi_{SC} = 0.472$
	Within sampled localities	80	54.274	0.678	14.07	$\Phi_{ST} = 0.859$
GENELAND clusters	Among clusters I, II, and III	2	68.464	1.108	50.04	$\Phi_{CT} = 0.500$
	Among sampled localities within clusters	17	45.902	0.428	19.32	$\Phi_{SC} = 0.387$
	Within sampled localities	80	54.274	0.678	30.64	$\Phi_{ST} = 0.694$
BARRIERS	Among barriers I, II, III, and IV	4	80.711	0.941	48.76	$\Phi_{CT} = 0.173$
	Among sampled localities within barriers	9	17.634	0.171	8.87	$\Phi_{SC} = 0.576$
	Within sampled localities	86	70.296	0.817	42.37	$\Phi_{ST} = 0.488$

The analysis was run independently using populations grouped by phylogenetic lineages (lineages A and B), by GENELAND clusters, and by the most supported geographic break, as identified by BARRIER analysis.
Φ_{CT}: genetic differentiation among groups.
Φ_{SC}: genetic differentiation among populations within groups.
Φ_{ST}: genetic differentiation among populations.

significant changes in population sizes (Ramos-Onsins & Rozas, 2002). The mismatch distribution of the whole sample suggests a recent history of population expansion, a scenario depicted by a typical unimodal and smooth distribution (Fig. 4A). The analysis revealed a non-significant SSD value (SSD = 0.006, $P = 0.123$) that did not refute the demographic model of spatial expansion for *Octodontomys gliroides* (Table 4). Also, the Harpending's raggedness index was not significant ($H = 0.029$, $P = 0.354$; Table 4). A pattern of demographic population expansion for lineages A and B was further supported by low and statistically non-significant Harpending's raggedness index and SSD values (Fig. 4C, E; Table 4). Expansion parameters (θ and τ), estimated under the spatial expansion model, are indicated in Table 4.

The demographic scenario for *Octodontomys gliroides* obtained through the BSPs suggested a dual pattern. In particular, a long history of constant population size followed by a period of a slight to moderate demographic expansion that occurred in the recent past. The time of expansion was estimated to have started in the Late Pleistocene, *c*. 0.05 Mya. After this population expansion, a recent decrease of effective population size (N_e) occurred *c.* 8 kya (Fig. 4B). The BSP analysis for lineage A showed a similar pattern with slight growth occurring over the last 0.04 Mya and a recent decrease of N_e beginning 10 kya (Fig. 4D). In contrast, the data for lineage B seem to reflect a pattern of stable population sizes through time (Fig. 4F).

DISCUSSION

Geographic barriers modelling the genetic structure of *Octodontomys gliroides*

Our analyses of the mtDNA CR, supported by the phylogenetic and parsimony network analysis, showed a structured pattern of geographic differentiation within *Octodontomys gliroides* with the occurrence of two well-defined evolutionary lineages. Lineage A is restricted to Bolivia and Chile, and lineage B is restricted mainly to Argentina. This phylogeographic pattern was also described for other vertebrate species such as the South American mouse opossum *Thylamys pallidior* (Thomas, 1902) (Braun *et al.*, 2005; Palma *et al.*, 2014). Based on BARRIER analysis, a boundary (barrier II; Fig. 2A, B) was placed by the Monmomier's algorithm, corroborating the separation of all Argentinian populations from the remaining Bolivian and Chilean populations with high bootstrap support. We observe that the upper end of this barrier separates the Bolivian populations Bo10 and Bo11 from the remaining populations, but with low bootstrap support (Fig. 2A, B). This boundary corresponded to the San Juan River, which is the largest river in the eastern Andes and it is the principal tributary of the Pilcomayo River (Fig. 5). The San Juan River originates in the high mountains near Jujuy, Argentina, and flows from northern Argentina to south-west Bolivia through differing environments. Additionally, Argentinian populations are separated from the Chilean group by

Downloaded from https://academic.oup.com/zoolinnean/article/178/2/410/2674316 by guest on 10 January 2021

Table 4. Genetic diversity estimates based on mitochondrial DNA control region sequences from lineages A and B

Group	*N*	*Hap*	*S*	*Hd* ± SD	π ± SD	Tajima's *D*		Fu's *Fs*		Mismatch distribution			
						D	*P* ($D_s < D_{obs}$)	*F*	*P* ($F_s < F_{obs}$)	r_H	SSD	θ	τ
Lineage A	93	20	19	0.91 ± 0.01	0.0043 ± 0.0026	−0.969	0.347 n.s.	−8.237	0.003	0.038 n.s.	0.004 n.s.	0.004	2.688
Lineage B	7	6	6	0.95 ± 0.09	0.0038 ± 0.0027	−0.536	0.353 n.s.	−3.027	0.008	0.107 n.s.	0.019 n.s.	0.01	2.248
TOTAL	100	26	24	0.92 ± 0.01	0.0059 ± 0.0034	−0.782	0.245 n.s.	−10.97	0.002	0.029 n.s.	0.006 n.s.	0.014	2.783

N, number of sequences; *Hap*, number of haplotypes; *S*, polymorphic sites; *Hd*, haplotype diversity; π, nucleotide diversity; r_H, Harpending's raggedness index; SSD, sum of squared deviations; n.s., non significant.

the occurrence of the Atacama Desert and by the high mountain ranges (>4800 m a.s.l.) found at the border of Chile and Argentina (see barrier III; Figs 2A, B and 5).

None of our analyses reproduced the different ecoregions where *Octodontomys gliroides* specimens were collected. Lineage A included individuals collected at the Andean Puna (northern, central, and southern Puna) and Andean pre-Puna. Lineage B included individuals from southern Andean Puna and Andean pre-Puna. Additionally, the genetic relationships among populations of *Octodontomys gliroides* increases with geographic distance, supporting an isolation by distance model, where the geographically close populations were characterized by low genetic differentiation, but when the distance among populations increased the genetic differentiation among populations also increased. In addition the comparison of N_{ST} and G_{ST} supported a phylogeographic structure in this species ($N_{ST} > G_{ST}$), and our results further suggest that closely related haplotypes are often found in the same area. This pattern of population differentiation was also supported by the results of the AMOVA ($P < 0.001$), which revealed that 73% of the overall mtDNA variation is accounted by differences between both lineages.

In turn, lineage A comprised two sublineages, A1 (widespread in northern Chile and in central and southern Bolivia) and A2 (restricted to northern and central Bolivia). This phylogenetic subdivision was supported by the parsimony network; however, this was very emergent separation because most haplotypes diverged in only one base pair (Fig. 1B). Two boundaries, consisting of one major boundary between these sublineages and one additional boundary within these sublineages, were detected by BARRIER analysis. A major barrier (see barrier I; Fig. 2A, B) separated the Chilean populations and Bolivian population Bo5 from the remaining Bolivian populations. In turn, the most northern (Bo1 and Bo2) and two central (Bo3 and Bo4) Bolivian populations were separated from neighbouring Bolivian populations (Bo6–Bo9). This separation is in agreement with the major barriers present in the area (i.e. major rivers, salt flats, the Atacama Desert, and the mountain chains of the Bolivian Andes). Lakes and river systems form an extensive endorheic basin constituted by the Titicaca and Poopó lakes, and by the Coipasa and Uyuni salt flats (Fig. 5). The major rivers connecting lakes and salt flats are the Desaguadero and the Lacajahuira. The Titicaca and the Poopó lakes are connected by the Desaguadero River that flows permanently, and the Lacajahuira River connects the Poopó Lake with the Coipasa salt flat (Fig. 5). The headwaters of these two permanent rivers increase during the wet season in the austral

Downloaded from https://academic.oup.com/zoolinnean/article/178/2/410/2674316 by guest on 10 January 2021

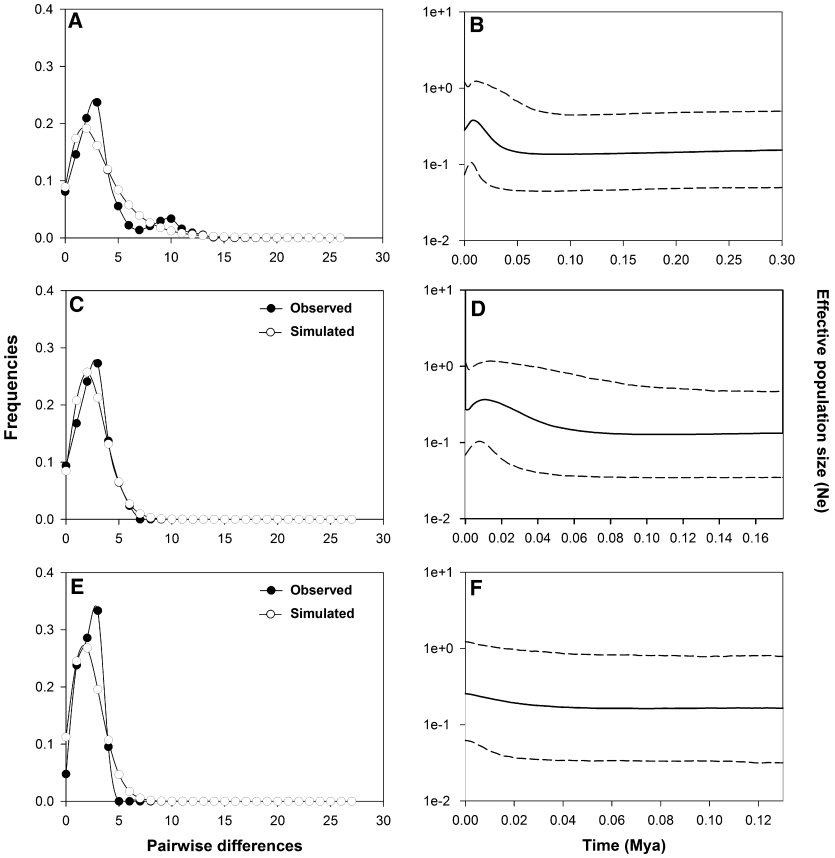

Figure 4. Pairwise mismatch distribution (left) and Bayesian skyline plots (right), depicting the demographic history for the entire sample (A and B), lineage A (C and D), and lineage B (E and F). For mismatch distributions, black circles represent the observed distribution of pairwise differences and white circles represent the theoretical expected distribution under a population expansion model. For the skyline plot, black lines represent median estimates, whereas the dotted lines represent the upper and lower 95% credible intervals. The *x*-axis of Bayesian skyline figures is the time per million years before the present and the *y*-axis is the estimated effective population size (N_e).

summer (Roche *et al.*, 1991). A critical characteristic of these two Andean rivers is that both are associated with large river–floodplain systems. In particular, the floodplain system of Desaguadero River undergoes strong floods when the water level increases in the Titicaca Lake, reaching a width of ~1 km. The floodplain is constituted by large sand deposits without vegetation, locally known as 'arenales'. Thus an additional boundary, corresponding to these river systems, was detected between the most northern Bolivian populations (Bo1 and Bo2) and the central Bolivian populations (Bo3 and Bo4, see barrier IV; Fig. 2A, B). An additional barrier that may have contributed to separating the northernmost and central Bolivian populations from the southern Bolivian populations is the 'Cordillera de los Frailes', a mountain range that borders the Poopó Lake in the north-west, and extends in to the south in the north-east of the department of Potosi, Bolivia (Montes de Oca, 2005; Fig. 5). Even though the presence of barriers such as rivers, highlands, salt flats, and the Atacama Desert seem to have had an important role in shaping the genetic differentiation between haplotypes and populations of this rodent species. The geographical distances among populations seems to be the main factor in shaping the genetic structure of the Andean degu.

The GENELAND analysis recovered three genetic clusters (Fig. 3A–D): (1) the northernmost and central Bolivian populations; (2) the Chilean populations, the central and southern Bolivian populations, and one Argentinian population; and (3) the remaining Argentinian populations and one southern Bolivian population. Cluster III exactly agreed with one of the lineages recognized in the phylogenetic and parsimony network analysis (lineage B). This cluster was separated from the other two clusters in the same area where Monmonier's algorithm inferred

Downloaded from https://academic.oup.com/zoolinnean/article/178/2/410/2674316 by guest on 10 January 2021

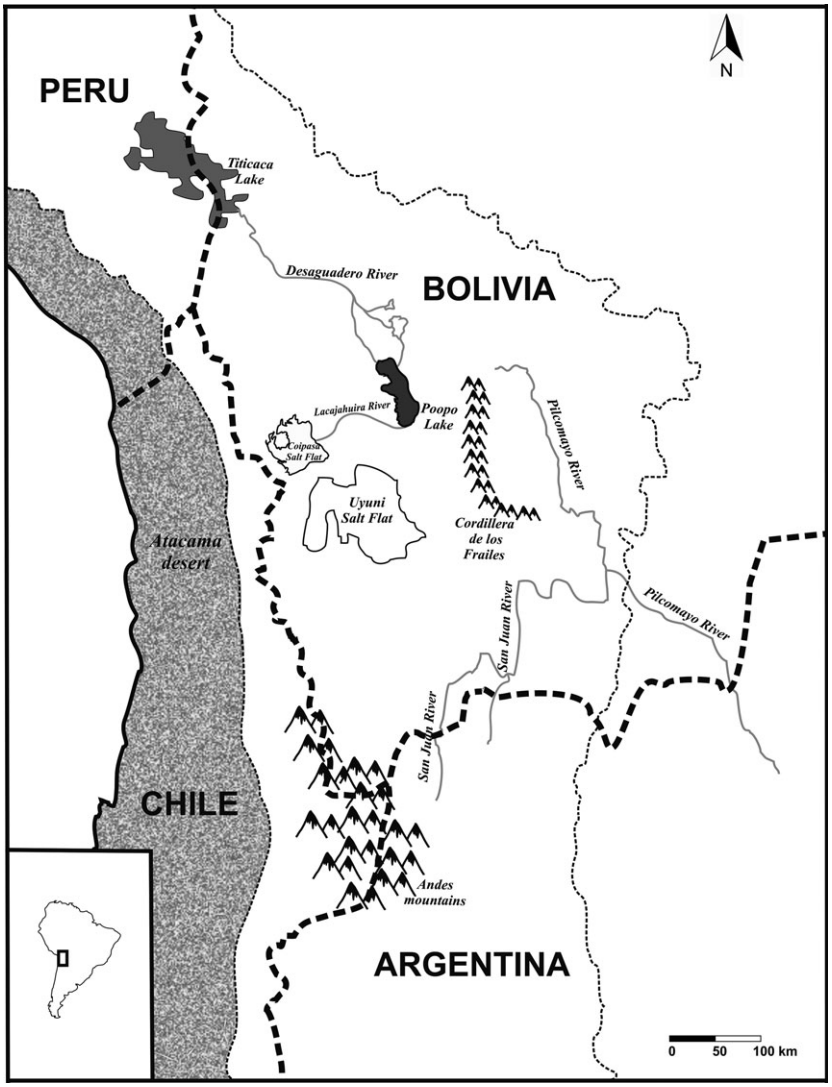

Figure 5. Map, showing the putative barriers (major rivers, lakes, salt flats, the Atacama Desert, and the mountain chains of the Andes) that separate the populations of *Octodontomys gliroides*.

the genetic barriers II and III to occur (Fig. 2A, B). The other two genetic clusters corresponded to lineage A (more precisely the sublineages A1 and A2). The genetic break between both sublineages was approximately at the same area where Monmonier's algorithm inferred the presence of barrier I (Fig. 2A, B).

Calibration estimates derived from the mtDNA CR suggest that the time to the most recent common ancestor for *Octodontomys gliroides* and its sister species *Octodon degus* was during the Late Miocene, *c*. 5.99 Mya, which is close to the 6.07 Mya estimated by Opazo (2005) using the *12S* rRNA gene; however, this calibration date is older than the 2.9–4.1 Mya reported by Honeycutt, Rowe & Gallardo (2003) using *12S* rRNA and the nuclear growth hormone receptor (*GHR*) gene. In addition, our estimates agreed with those based on DNA hybrization (5.0–7.0 Mya; Gallardo & Kirsch, 2001). On the other hand, our results indicated that the diversification between the highly divergent lineages of the *Octodontomys gliroides* (lineage A and lineage B) occurred during the Middle Pleistocene 0.69 Mya, followed by further diversification events within each lineage (Fig. 1A). The estimated diversification time for lineage A was found to be *c.* 0.350 Mya, followed by lineage B at 0.20 Mya. These calibration times for the *Octodontomy*s lineages are surprisingly low estimates given the records for other octodontid rodents: *c*. 1.47 Mya for *Tympanoctomys barrerae* (Gallardo *et al.*, 2013) and *c*. 1.25 Mya for *Octodon degus* (Valladares, 2009). Our estimate is not in disagreement

Downloaded from https://academic.oup.com/zoolinnean/article/178/2/410/2674316 by guest on 10 January 2021

with palaeontological data. In fact, this period agrees with a time of active orogenesis and substantial global climate fluctuations (i.e. dramatic oscillations in precipitation, see below) in the Andean region by the Late Pliocene–Pleistocene (Placzek *et al.*, 2009, 2011). These biogeographic events may have allowed the formation of new environments for the differentiation of local biota such as the Andean Altiplano (Puna) and the Atacama Desert (Palma, Marquet & Boric-Bargetto, 2005; Lougheed *et al.*, 2013; Álvarez-Varas, González-Acuña & Vianna, 2015). Our results are also concordant with examples of other vertebrate taxa that show similar diversification patterns: Andean passerine birds of the genus *Phrygilus* (Álvarez-Varas *et al.*, 2015), the Rofous-collared sparrow *Zonotrichia capensis* (Müller, 1776) (Lougheed *et al.*, 2013), and sigmodontine taxa of the genus *Phyllotis* (Palma *et al.*, 2005), sculpted by changes associated with the geological and environmental history of the High Andes region during the Pleistocene, in particular with periods of contraction and expansion in what are known as palaeolakes (see below). Thus the ages presented in this paper can be regarded as rough estimations of diversification times for this species, which are now available for future comparisons and evaluation. Assessment of other mitochondrial and nuclear loci might corroborate the data presented in this study.

Demographic history

Our genetic diversity analyses revealed high haplotype diversity for both lineages of *Octodontomys gliroides*, although relatively low nucleotide diversity for each of them (Table 4). These results suggest recent differentiation with rapid population growth (Grant & Bowen, 1998). A similar pattern of nucleotide and haplotype diversity has been reported for populations of *Octodon degus* (Valladares, 2009), *Spalacopus cyanus* (Opazo *et al.*, 2008), and *Tympanoctomys barrerae* (Ojeda, 2010; Gallardo *et al.*, 2013). This pattern of genetic variability suggests population growth following a period of decreased effective population size (N_e) (Grant & Bowen, 1998; Avise, 2000; Cope, 2004). Low genetic divergence among most populations of *Octodontomys gliroides* (i.e. low values of nucleotide diversity among haplotypes) supports the hypothesis that colonization into recently available ranges occurred rapidly (Grant & Bowen, 1998; Palma *et al.*, 2012). Our analyses are consistent with a history of long-term demographic stability for *Octodontomys gliroides* in most of its current distributional range. Neutrality tests indicated that the demographic histories of some areas differed, suggesting that *Octodontomys gliroides* has experienced different demographic events in the recent past. In this way we observed signals of recent demographic expansion for the whole samples and for lineage A, whereas lineage B seems to reveal a signal of stability (Table 4). This apparent stability could be generated by a lack of statistical power, caused by the low sample size ($N = 7$). BSP analysis based on a population sample of only a few individuals often fails to capture a population expansion when it has occurred (Grant, 2015). As in our case, a flat curve in BSP analysis was interpreted as indicative of long-term population stability. The small sample size probably led to a widespread underestimation of the magnitude of population expansions in lineage B. However, it could reflect a loss of information during population fluctuations (Grant, 2015).

Although a sample size of individuals greatly affects the power of the demographic reconstructions yielded by BSP analysis, a small sample size does not appear to diminish the usefulness of mismatch analysis (Grant, 2015). The mismatch distribution for the entire sample level was unimodal (Fig. 4A), and the negative values for both Tajima's D and Fu's F_S tests supported demographic expansion, with the latter test showing statistical significance (Table 4). In addition, the same scenario was also supported by non-significant SSD and raggedness values (Table 4). Our observations of non-significant values in goodness-of-fit distribution for the entire sample level and lineage A suggest that population expansion occurred recently (Rogers, 1995). The BSP analysis corroborated this pattern, showing that the N_e of *Octodontomys gliroides* remained constant until *c.* 0.05 Mya (Late Pleistocene; Fig. 4B), when a moderate period of population expansion began. After this population expansion, a recent decrease of N_e occurred *c.* 8 kya. Similarly, the demographic analyses for lineage A showed that after a long time of constant population size, slight growth occurred over the last 0.04 Myr, with a recent decrease of N_e beginning 10 kya. This demographic expansion was associated with major climatic changes that occurred during the wet–dry events of the Pleistocene at the Andean Puna region (Placzek *et al.*, 2009; see below). Although a signal of population range expansion was detected for lineage B (unimodal mismatch distribution, statistically significant values for Fu's F_S-test, and non-significant SSD test), this pattern remained unclear after BSP analysis, probably through the effect of a limited sample size (Fig. 4F, see above). Most importantly, however, our results are in agreement with evidence from other octodontids: Valladares (2009) and Gallardo *et al.* (2013) reported recent population expansion in *Octodon degus* (0.25 Mya) and *Tympanoctomys barrerae* (0.05–0.1 Mya), respectively, and other Andean vertebrates have also shown an

Downloaded from https://academic.oup.com/zoolinnean/article/178/2/410/2674316 by guest on 10 January 2021

expansion signature at *c*. 0.6 Mya in the Highlands (*Phrygilus plebejus* Tschudi, 1844; Álvarez-Varas *et al.*, 2015).

Biogeographic scenario

Records of major climatic changes affecting the Andean Puna region during the wet–dry events of the Pleistocene (Placzek *et al.*, 2009) may shed light on understanding the patterns of demographic expansion experienced by populations of *Octodontomys gliroides*. At least three major events associated with dramatic changes in precipitation have been reported for the Andean Puna during the last 0.12 Myr (Risacher & Fritz, 2000; Placzek *et al.*, 2011), which have been associated with important changes in the biota of the area (Placzek *et al.*, 2009) and in the primary habitat of *Octodontomys gliroides*. During this period, climatic oscillations contributed to the formation of large palaeolakes (there was an increase in annual precipitation of 30–50%) that covered the endorheic basin of the Titicaca and Poopó lakes, and the Coipasa and the Uyuni salt flats, between 0.12 and 0.08 Mya (Placzek *et al.*, 2009, 2013). Potential causes for these climate changes may be linked to interannual and millenial variation in tropical Pacific sea-surface temperature gradients (Garreaud, Vuille & Clement, 2003; Cane, 2005), and to the North Atlantic sea-surface temperature and moisture arriving in the central Andean Puna (Placzek *et al.*, 2013). The first maximum palaeolake expansion of Ouki-Salinas started about 0.12 Mya and ended about 0.08 Mya (Placzek *et al.*, 2013), with ~80 m of depth (Placzek *et al.*, 2009). After this period, the lake retreated and the Andean Puna environments became relatively dry and cold during the next 0.04 Myr (Placzek, Quade & Patchett, 2006). Later, a new shorter wet period took place around 0.02 Mya, with the formation of the Tauca lake cycle, that reached a maximum around 0.015 Mya, resulting in the deepest (~140 m) and largest lake in the basin over the past 0.12 Myr (Placzek *et al.*, 2009). The last period is known as the Coipasa lake cycle, with ages between 0.013 and 0.011 Mya (Placzek *et al.*, 2006), and both the Tauca and the Coipasa lake cycles are referred to as the Central Andean Pluvial Event (CAPE) (Quade *et al.*, 2008; Placzek *et al.*, 2009).

Our results support the biogeographic scenario described above, with a relatively stable population size for major lineages of *Octodontomys gliroides* during the Ouki lake cycles, and with a posterior moderate population growth starting around 0.05 Mya, in agreement with a dry-wet stable period. After this population expansion, a relatively recent decrease of population size occurred during the CAPE phase (*c.* 0.015 Mya). This pattern of expansion and recent decrease was evident for the whole sample and for lineage A. Interestingly, the expansion of populations agreed with the inter-lake time of 0.08–0.025 Mya, which was the longest period of dry conditions in the Andean Puna in the last 1.3 Myr (Placzek *et al.*, 2013). Past hydrologic change recorded in two sediment cores (Fornari, Risacher & Feraud, 2001; Chepstow-Lusty *et al.*, 2005) evidenced an increase in vegetation species, with the presence of *Polylepis*/Acaena pollen and a high abundance of *Asteraceae*, *Chenopodiaceae*, *Cyperaceae, Myriophyllum*, and *Pediastrum* during this period. Additional evidence for wet events from the central Andean region come from the higher percentage of grass abundance reported from rodent middens (including *Octodontomys gliroides*; Latorre *et al.*, 2002; Placzek *et al.*, 2009). The canyons or 'quebradas' formed during these periods have been postulated as biotic corridors extending from the Puna to pre-Puna areas (Palma *et al.*, 2005).

Taken as a whole, the information presented in this paper is, to our knowledge, the first attempt to assess the phylogeography of the scarcely known Andean degu over its entire range distribution, yielding important insights into the evolutionary history and current changes in levels of gene flow of this species.

ACKNOWLEDGEMENTS

We thank F. Alfaro, G. Villanueva, H. Villca, M. Orellana, A. Coca, and O. Osco for their assistance during data collection. We thank R. Ojeda, A. Ojeda, P. Jayat, D. Flores, and R. Sobrero for providing tissue samples. We also wish to thank the following institutions who collaborated with the shipping and loan of tissue and skin samples: Field Museum of Natural History; Sam Noble Oklahoma Museum of Natural History; Instituto de Ecología y Evolución, Universidad Austral de Chile; Colección de Flora y Fauna Profesor Patricio Sánchez Reyes, P. Universidad Católica de Chile; Museo Municipal de Ciencias Naturales 'Lorenzo Scaglia' and Colección de Mamíferos del Instituto Argentino de Investigaciones de zonas Áridas (IADIZA). D.S.R. is really grateful to the people from the Laboratory of Evolutionary Biology of Prof. E. Palma, and R. Cancino and M. Manzano, for assistance in the laboratory. D.S.R. is also thankful to A. Parada for his assistance with molecular analyses. We thank the Dirección General de Biodiversidad, Bolivia and Servicio Agrícola y Ganadero, Chile, for trapping permits in Bolivia and Chile, respectively. The Centro de Biodiversidad y Genética- Universidad Mayor de San Simón and Laboratorio de Ecología Conductual,

Downloaded from https://academic.oup.com/zoolinnean/article/178/2/410/2674316 by guest on 10 January 2021

Departamento de Ecología-Pontificia Universidad Católica (PUC) provided traps and field equipment. We also appreciate the helpful comments made by two anonymous reviewers that significantly improved the article. D.S.R. was supported by the Organización de los Estados Americanos (OEA), Comisión Nacional Científica y Tecnológica (CONICYT), Vicerrectoría de Investigación, and Dirección de Investigación y Postgrado-PUC (VRI-UC and DIP-UC), the Animal Behaviour Society (Student Research Awards and Developing Nations Research Grant), the American Society of Mammalogists, the Program 1 of Centro de Estudios Avanzados en Ecología y Biodiversidad (FONDO Nacional de Desarrollo de áreas Prioritarias # 1501–001), and Fondo Nacional de Ciencias y Tecnología (FONDECYT; grant no. 3140395). L.A.E. and R.E.P. were supported by FONDECYT grants (nos 1090302 and 1100558, and no. 1130467, respectively).

REFERENCES

Aagesen L, Szumik CA, Zuloaga FO, Morrone O. 2009. Quantitative biogeography in the South America highlands —recognizing the Altoandina, Puna and Prepuna through the study of Poaceae. *Cladistics* **25:** 295–310.

Álvarez-Varas R, González-Acuña D, Vianna JA. 2015. Comparative phylogeography of co-distributed *Phrygilus* species (Aves, Thraupidae) from the Central Andes. *Molecular Phylogenetics and Evolution* **90:** 150–163.

Animal Care and Use Committee. 1998. Guidelines for the capture, handling, and care of mammals as approved by the American Society of Mammalogists. *Journal of Mammalogy* **79:** 1416–1431.

Avise JC. 2000. *Phylogeography: the history and formation of species*. Cambridge, Massachusetts: Harvard University Press.

Beck SG. 1985. Flórula ecológica de Bolivia**:** Puna semiárida en el Altiplano Boliviano. *Ecología en Bolivia* **6:** 1–41.

Braun JK, Van Den Bussche RA, Morton PK, Mares MA. 2005. Phylogenetic and biogeographic relationships of mouse opossums *Thylamys* (Didelphimorphia, Didelphidae) in southern South America. *Journal of Mammalogy* **86:** 147–159.

Brown GG. 1986. Structural conservation and variation in the D-loop-containing region of vertebrate mitochondrial DNA. *Journal of Molecular Biology* **192:** 503–511.

Cabrera AL. 1968. Ecología vegetal de la Puna. *Colloquium Geographicum* **9:** 91–116.

Cabrera AL, Willink AW. 1973. Biogeografía de América Latina Serie de Biología OEA. *Monografía* **13:** 1–117.

Cane MA. 2005. The evolution of El Niño, past and future. *Earth and Planetary Science Letters* **230:** 227–240.

Chepstow-Lusty A, Bush MB, Frogley MR, Baker PA, Fritz SC, Aronson J. 2005. Vegetation and climate change on the Bolivian Altiplano between 108 000 and 18 000 yr ago. *Quaternary Research* **63:** 90–98.

Clement M, Posada D, Crandall KA. 2000. TCS: acomputer program to estimate gene genealogies. *Molecular Ecology* **9:** 1657–1659.

Contreras LC, Torres-Mura JC, Yánez JL. 1987. Biogeography of octodontid rodents**:** an eco-evolutionary hypothesis. *Fieldiana Zoology* **39:** 401–411.

Cope JM. 2004. Population genetics and phylogeography of the blue rockfish (*Sebastes mystinus*) from Washington to California. *Canadian Journal of Fisheries and Aquatic Sciences* **61:** 332–342.

Davis SD, Heywood VH, Herrera-MacBryde O, Villa-Lobos J, Hamilton AC. 1997. Altoandina Argentina, Chile. In: Davis SD, Heywood VH, Herrera-MacBryde O, Villa-Lobos J, Hamilton AC, eds. *Centres of plant diversity: A guide and strategy for their conservation*. Oxford, UK: IUCN, WWF.

Drummond AJ, Rambaut A, Shapiro B, Pybus OG. 2005. Bayesian coalescent inference of past population dynamics from molecular sequences. *Molecular Biology and Evolution* **22:** 1185–1192.

Drummond AJ, Ho SYW, Phillips MJ, Rambaut A. 2006. Relaxed phylogenetics and dating with confidence. *PLoS Biology* **4:** e88.

Drummond AJ, Suchard MA, Xie D, Rambaut A. 2012. Bayesian phylogenetics with BEAUti and the BEAST 1.7. *Molecular Biology and Evolution* **13:** 1969–1973.

Dupanloup I, Schneider S, Excoffier L. 2002. A simulated annealingapproach to define the genetic structure of populations. *Molecular Ecology* **11:** 2571–2581.

Ebensperger LA, Cofré H. 2001. On the evolution of group-living in the New World cursorial hystricognath rodents. *Behavioral Ecology* **12:** 227–236.

Excoffier L. 2004. Patterns of DNA sequence diversity and genetic structure after a range expansion: lessons from the infinite-island model. *Molecular Ecology* **13:** 853–864.

Excoffier L, Lischer HEL. 2010. Arlequin suite ver 3.5: a new series of programs to perform population genetics analyses under Linux and Windows. *Molecular Ecology Resources* **10:** 564–567.

Fontanella FM, Feldman CR, Siddall ME, Burbrink FT. 2008. Phylogeography of *Diadophis punctatus*: Extensive lineage diversity and repeated patterns of historical demography in a trans-continental snake. *Molecular Phylogenetics and Evolution* **46:** 1049–1070.

Fornari M, Risacher F, Feraud G. 2001. Dating paleolakes in the central Altiplano of Bolivia. *Palaeogeography, Palaeoclimatology, Palaeoecology* **172:** 269–282.

Fu YX. 1997. Statistical tests of neutrality of mutations against population growth, hitchhiking and background selection. *Genetics* **147:** 915–925.

Gallardo MH, Kirsch JAW. 2001. Molecular relationships among octodontidae (Mammalia: Rodentia: Caviomorpha). *The Journal of Mammalian Evolution* **8:** 73–89.

Gallardo MH, Ojeda RA, González CA, Ríos CA. 2007. The Octodontidae revised. In: Kelt DA, Lessa EP, Salazar-Bravo J, Patton JL, eds. *The quintessential naturalist: honoring the life and legacy of Oliver P. Pearson*, *Vol. 134*. Berkeley, CA: University of California Publications in Zoology, 1–988.

Downloaded from https://academic.oup.com/zoolinnean/article/178/2/410/2674316 by guest on 10 January 2021

Gallardo MH, Suárez-Villota EY, Nuñez JJ, Vargas RA, Haro R, Köhler N. 2013. Phylogenetic analysis and phylogeography of the tetraploid rodent *Tympanoctomys barrerae* (Octodontidae): insights on its origin and the impact of Quaternary climate changes on population dynamics. *The Biological Journal of the Linnean Society* **108:** 453–469.

Garreaud RD, Vuille M, Clement AC. 2003. The climate of the Altiplano: observed current conditions and mechanisms of past changes. *Palaeogeography, Palaeoclimatology, Palaeoecology* **194:** 5–22.

Gervais P, d'Orbigny D. 1844. Nouveau bulletin des sciences par la Société Philomatique, Paris.

Grant WS. 2015. Problems and cautions with sequence mismatch analysis and bayesian skyline plots to infer historical demography. *Journal of Heredity*. doi:10.1093/jhered/esv020.

Grant WAS, Bowen BW. 1998. Shallow population histories in deep evolutionary lineages of marine fishes: insights from sardines and anchovies and lessons for conservation. *Journal of Heredity* **89:** 415–426.

Guillot G, Estoup A, Mortier F, Cosson JF. 2005a. A spatial statistical model for landscape genetics. *Genetics* **170:** 1261–1280.

Guillot G, Mortier F, Estoup A. 2005b. Geneland: a computer package for landscape genetics. *Molecular Ecology Notes* **5:** 712–715.

Guillot G, Renaud S, Ledevin R, Michaux J, Claude J. 2012. A unifying model for the analysis of phenotypic, genetic, and geographic data. *Systematic Biology* **61:** 897–911.

Hammer Ø, Harper DAT, Ryan PD. 2001. PAST: Paleontological statistics software package for education and data analysis. *Palaeontologia Electronica* **4:** 9pp http://palaeo-electronica.org/2001_1/past/issue1_01.htm.

Harpending HC. 1994. Signature of ancient population growth in a low resolution mitochondrial DNA mismatch distribution. *Human Biology* **66:** 591–600.

Honeycutt RL, Rowe DL, Gallardo MH. 2003. Molecular systematics of the South American Caviomorph rodents: relationships among species and genera in the family Octodontidae. *Molecular Phylogenetics and Evolution* **26:** 476–489.

Hutterer R. 1994. Island rodents**:** a new species of *Octodon* from Isla Mocha, Chile (Mammalia: Octodontidae). *Zeitschrift für Säugetierkunde* **59:** 27–51.

Keane TM, Creevey CJ, Pentony MM, Naughton TJ, McInerney JO. 2006. Assessment of methods for amino acid matrix selection and their use on empirical data shows that ad hoc assumptions for choice of matrix are not justified. *BMC Evolutionary Biology* **6:** 29.

Lacey EA, Ebensperger LA. 2007. Social structure in Octodontid and Ctenomyid rodents. In: Wolff JO, Sherman PW, eds. *Rodent societies an ecological and evolutionary perspective*. Chicago, IL: University of Chicago Press, 257–296.

Latorre C, Betancourt JL, Rylander KA, Quade J. 2002. Vegetation invasions into Absolute Desert: A 45 000-yr rodent midden record from the Calama-Salar de Atacama Basins, northern Chile (22-24°S). *Geological Society of America Bulletin* **114:** 349–366.

Lawrence B. 1941. A new species of *Octomys* from Argentina. *Proceedings of the New England Zoölogical Club* **18:** 43–46.

Librado P, Rozas J. 2009. DnaSP v5: a software for comprehensive analysis of DNA polymorphism data. *Bioinformatics* **25:** 1451.

López RP, Beck SG. 2002. Phytogeographical affinities and life form composition of the Bolivian Prepuna. *Candollea* **57:** 77–96.

Lougheed SC, Campagna L, Dávila JA, Tubaro PL, Lijtmaer DA, Handford P. 2013. Continental phylogeography of an ecologically and morphologically diverse Neotropical songbird. Zonotrichia capensis. *BMC Evolutionary Biology* **13:** 58.

Manni F, Guérard E, Heyer E. 2004. Geographic patterns of (genetic, morphologic, linguistic) variation: how barriers can be detected by usingMonmonier's algorithm. *Human Biology* **76:** 173–190.

Mantel N. 1967. The detection of disease clustering and a generalized regression approach. *Cancer Research* **27:** 209–220.

Mares MA, Ojeda RA. 1982. Patterns of diversity and adaptation in South American hystricognath rodents. In: Mares MA, Genoways HH, eds. *Mammalian biology in South America*, *Vol. 6*. Special Publication Series, Pymatuning Laboratory of Ecology. Pittsburgh, PA: University of Pittsburgh, 1–539.

Mares MA, Braun JK, Barquez RM, Díaz MM. 2000. Two new genera and species of halophytic desert mammals from isolated salt flats in Argentina. *Museum of Texas Tech University* **203:** 1–27.

Molina GI. 1782. *Saggio sulla storia naturale del Chile*. Bologna: Auino.

Montes de Oca I. 2005. *Enciclopedia Geográfica de Bolivia*. La Paz: Atenea.

Nei M, Kumar S. 2000. *Molecular evolution and phylogenetics*. Oxford: Oxford University Press.

Nester PL, Gayó E, Latorre C, Jordan TE, Blanco N. 2007. Perennial stream discharge in the hyperarid Atacama Desert of northern Chile during the latest Pleistocene. *Proceedings of the National Academy of Sciences* **104:** 19724–19729.

Ojeda AA. 2010. Phylogeography and genetic variation in the South American rodent *Tympanoctomys barrerae* (Rodentia: Octodontidae). *Journal of Mammalogy* **91:** 302–313.

Ojeda RA, Blendinger PG, Brandl R. 2000. Mammals in South American Drylands: Faunal Similarity and Trophic Structure. *Global Ecology and Biogeography* **9:** 115–123.

Ojeda AA, Novillo A, Ojeda RA, Roig-Juñent S. 2013. Geographical distribution and ecological diversification of South American octodontid rodents. *Journal of Zoology* **289:** 285–293.

Opazo JC. 2005. A molecular timescale for Caviomorph rodents (Mammalia, Hystricognathi). *Molecular Phylogenetics and Evolution* **37:** 932–937.

Opazo JC, Bugueño MP, Carter MJ, Palma RE, Bozinovic F. 2008. Phylogeography of the subterranean rodent

Downloaded from https://academic.oup.com/zoolinnean/article/178/2/410/2674316 by guest on 10 January 2021

Spalacopus cyanus (Caviomorpha, Octodontidae). *Journal of Mammalogy* **89:** 837–844.

Osgood WH. 1943. The mammals of Chile. *Field Museum of Natural History. Zoological series* **30:** 1–268.

Palma RE, Marquet PA, Boric-Bargetto D. 2005. Inter- and intraspecific phylogeography of small mammals in the Atacama Desert and adjacent areas of northern Chile. *Journal of Biogeography* **32:** 1931–1941.

Palma RE, Boric-Bargetto D, Torres-Pérez F, Hernández CE, Yates TL. 2012. Glaciation effects on the phylogeographic structure of *Oligoryzomys longicaudatus* (Rodentia**:** Sigmodontinae) in the Southern Andes. *PLoS ONE* **7:** e32206.

Palma RE, Boric-Bargetto D, Jayat JP, Flores DA, Zeballos H, Pacheco V, Cancino RA, Alfaro FD, Rodríguez-Serrano E, Pardiñas UF. 2014. Molecular phylogenetics of mouse opossums: new findings on the phylogeny of *Thylamys* (Didelphimorphia, Didelphidae). *Zoologica Scripta* **43:** 217–234.

Pearson OP. 1984. Taxonomy and natural history of some fossorial rodents of Patagonia, southern Argentina. *Journal of Zoology* **202:** 225–237.

Placzek C, Quade J, Patchett PJ. 2006. Geochronology and stratigraphy of late Pleistocene lake cycles on the southern Bolivian Altiplano: Implications for causes of tropical climate change. *Geological Society of America Bulletin* **118:** 515–532.

Placzek C, Quade J, Betancourt JL, Patchett PJ, Rech JA, Latorre C, Matmon A, Homgren C, English NB. 2009. Climate in the Dry Central Andes over geologic, millennial, and interannual timescales 1. *Annals of the Missouri Botanical Garden* **96:** 386–397.

Placzek CJ, Quade J, Patchett PJ. 2011. Isotopic tracers of paleohydrologic change in large lakes of the Bolivian Altiplano. *Quaternary Research* **75:** 231–244.

Placzek CJ, Quade J, Patchett PJ. 2013. A 130 ka reconstruction of rainfall from the Bolivian Altiplano. *Earth and Planetary Science Letters* **363:** 97–108.

Pons O, Petit RJ. 1995. Estimation, variance and optimal sampling of gene diversity. *Theoretical and Applied Genetics* **90:** 462–470.

Pons O, Petit RJ. 1996. Measwring and testing genetic differentiation with ordered versus unordered alleles. *Genetic* **144:** 1237–1245.

Quade J, Rech JA, Betancourt JL, Latorre C, Fisher T. 2008. Paleowetlands and regional climate change in the central Atacama Desert, northern Chile. *Quaternary Research* **69:** 343–360.

Rambaut A. 2010. FigTree 1.3.1. Available from http://tree.bio.ed.ac.uk/software/figtree.

Rambaut A, Drummond AJ. 2009. Tracer v1.5. Available from http://beast.bio.ed.ac.uk/Tracer.

Ramos-Onsins SE, Rozas J. 2002. Statistical properties of new neutrality tests against population growth. *Molecular Biology and Evolution* **19:** 2092–2100.

Reig OA. 1981. *Teoría del Origen y Desarrollo de la Fauna de Mamíferos de América del Sur*. Monographie Naturae. Mar del Plata: Museo Municipal de Ciencias Naturales 'Lorenzo Scaglia', 162 p.

Reig OA. 1986. Diversity patterns and differentiation of High Andean Rodents. In: Vuilleumier F, Monasterio M, eds. *High altitude tropical biogeography*. New York y Oxford: Oxford University Press, 404–439.

Risacher F, Fritz B. 2000. Bromine geochemistry of Salar de Uyuni and deeper salt crusts, central Altiplano, Bolivia. *Chemical Geology* **167:** 373–392.

Rivera DS, Abades S, Alfaro FD, Ebensperger LA. 2014. Sociality of *Octodontomys gliroides* and other octodontid rodents reflects the influence of phylogeny. *Journal of Mammalogy* **95:** 968–980.

Roche MA, Bourges J, Cortes J, Mattos R. 1991. TV. 1 Climatología e hidrología de la cuenca del lago Titicaca. El Lago Titicaca: síntesis del conocimiento limnológico actual. Paris, 83–104.

Rogers AR. 1995. Genetic evidence for a Pleistocene population expansion. *Evolution* **49:** 608–615.

Rogers AR, Harpending H. 1992. Population-growth makes waves in the distribution of pairwise genetic-differences. *Molecular Biology and Evolution* **9:** 552–569.

Sambrook J, Fritsch EF, Maniatis T. 1989. *Molecular cloning*. New York: Cold spring harbor laboratory Press, 14–19.

Sikes RS, Gannon WL. 2011. Guidelines of the American Society of Mammalogists for the use of wild mammals in research. *Journal of Mammalogy* **92:** 235–253.

Tajima F. 1989. Statistical Method for Testing the Neutral Mutation Hypothesis by DNA Polymorphism. *Genetics* **123:** 585–595.

Thomas O. 1902. On Marmosa mamota and elegans, with descriptions of new subspecies of the latter. *Annals and Magazine of Natural History Series 7* **10:** 158–162.

Thomas O. 1917. A new species of *Aconaemys* from southern Chile. *Annals and Magazine of Natural History* **19:** 281–282.

Thomas O. 1920. On mammals from near Tinogasta, Catamarca, collected by Sr. Budin. *Annals and Magazine of Natural History* **9:** 117–119.

Valladares JP. 2009. Variación geográfica de la conducta antidepredatoria del *Octodon degus* (Molina 1782) bajo un contexto filogeográfico. Unpublished D. Phil. Thesis, Universidad de Chile.

Verzi DH, Quintana CA. 2005. The caviomorph rodents from the San Andrés formation, east-central Argentina, and global Late Pliocene climatic change. *Palaeogeography, Palaeoclimatology, Palaeoecology* **219:** 303–320.

Villesen P. 2007. FaBox**:** an online toolbox for fasta sequences. *Molecular Ecology Notes* **7:** 965–968.

Waterhouse GR. 1842 [1841]**.** Report of the meeting of November 9, 1841. *Proceedings of the Zoological Society of London* **1841:** 89–92.

Waterhouse GR. 1845 [1844]**.** On various skins of mammalian from Chile, with notes relating to them by Mr. Bridges. *Proceedings of the Zoological Society of London* **12:** 153–157.

Woods CA, Kilpatrick CW. 2005. Infraorder Hystricognathi. In: Wilson DE, Reeder DM, eds. *Mammal Species of the World: a taxonomic and geographic reference*. Baltimore: John Hopkins University Press, 1538–1600.

Downloaded from https://academic.oup.com/zoolinnean/article/178/2/410/2674316 by guest on 10 January 2021

APPENDIX 1

Polymorphic sites within mtDNA control region sequences for each haplotype of *Octodontomys gliroides*. Haplotype number and GenBank accession numbers are shown.

	Position of polymorphic sites																								
Haplotype no.	1	2	4	5	14	39	58	63	66	90	105	111	139	144	147	148	150	153	162	185	197	234	272	462	GenBank accession no.
H1	C	T	T	A	A	T	C	T	G	A	A	C	G	A	A	T	T	A	T	G	C	A	T	G	KF917586
H2	.	.	.	.	T	C	.	.	.	.	.	.	.	.	.	.	.	.	.	A	.	.	.	.	KF917587
H3	.	.	.	.	.	C	.	.	.	.	.	.	.	.	.	.	.	.	.	A	.	.	.	.	KF917588
H4	T	C	C	G	.	C	.	.	A	G	.	T	.	.	.	C	.	.	.	A	.	.	C	A	KF917589
H5	.	.	.	.	.	C	.	.	A	G	.	.	.	.	.	.	.	.	.	A	T	.	.	A	KF917590
H6	.	.	.	.	.	C	.	.	A	G	.	.	.	.	.	.	.	.	.	A	.	.	.	.	KF917591
H7	.	.	.	.	.	C	.	.	A	G	.	.	.	G	.	.	.	.	.	A	T	.	.	.	KF917592
H8	.	.	.	.	.	C	.	.	A	G	.	.	.	.	.	C	.	.	.	A	.	.	.	.	KF917593
H9	.	.	.	.	.	C	.	.	A	G	.	.	.	.	.	.	.	.	.	A	T	.	.	.	KF917594
H10	.	.	.	.	.	C	.	.	A	.	.	.	.	.	.	.	.	.	.	A	.	.	.	.	KF917595
H11	T	.	C	G	.	C	.	.	A	G	.	T	.	.	.	C	.	.	.	A	T	G	C	A	KF917596
H12	.	.	.	.	.	C	.	.	A	G	.	.	.	.	.	.	C	.	.	A	T	.	.	.	KF917597
H13	.	.	.	.	.	C	.	.	A	G	.	T	.	.	.	.	.	.	.	A	.	.	.	.	KF917598
H14	.	.	.	.	.	.	.	.	A	.	.	.	.	.	.	.	.	.	.	A	.	.	.	.	KF917599
H15	T	.	C	.	.	C	.	.	A	.	.	.	.	.	.	.	.	.	.	A	.	.	.	.	KF917600
H16	T	.	C	G	.	C	.	.	A	G	.	T	A	.	.	C	.	.	.	A	T	.	C	A	KF917601
H17	T	C	C	G	.	C	.	.	A	G	.	T	A	.	.	C	.	.	C	A	T	.	C	A	KF917602
H18	T	.	C	G	.	C	.	.	A	.	.	T	A	.	.	C	.	.	.	A	T	.	C	A	KF917603
H19	T	.	C	G	.	C	.	.	A	G	.	T	.	.	.	C	.	.	.	A	T	.	C	A	KF917604
H20	.	.	.	.	.	C	T	.	A	G	.	.	.	.	.	.	.	.	.	A	T	.	.	.	KF917605
H21	T	.	.	.	.	C	.	C	A	.	G	.	.	.	.	.	.	.	.	A	.	.	.	.	KF917606
H22	.	.	.	.	.	C	.	.	A	.	.	.	.	.	.	.	.	.	.	A	.	.	.	A	KF917607
H23	T	.	.	.	.	C	.	.	A	.	G	.	.	.	.	.	.	.	.	A	.	.	.	.	KF917608
H24	.	.	.	.	.	C	.	.	A	.	.	.	.	.	G	.	.	.	.	A	.	.	.	.	KF917609
H25	.	.	.	.	.	C	.	.	A	.	G	.	.	.	.	.	.	.	.	A	.	.	C	.	KF917610
H26	.	.	.	.	.	C	.	C	A	.	.	.	.	.	.	.	C	G	.	A	.	.	.	.	KF917611

Downloaded from https://academic.oup.com/zoolinnean/article/178/2/410/2674316 by guest on 10 January 2021

APPENDIX 2

Haplotypes and their frequencies in each ecogeographic ecoregion.

	Ecoregions				
	Andean Puna				
Haplotype	Northern Puna	Central Puna	Southern Puna	Andean pre-Puna	Total
H1	–	–	–	3	3
H2	–	–	–	5	5
H3	–	5	7	2	14
H4	–	–	–	1	1
H5	–	4	–	–	4
H6	4	3	–	–	7
H7	–	5	–	–	5
H8	–	5	10	–	15
H9	3	1	–	–	4
H10	–	1	3	13	17
H11	–	–	1	–	1
H12	4	–	–	–	4
H13	1	–	–	–	1
H14	–	–	–	2	2
H15	–	–	–	1	1
H16	–	–	–	1	1
H17	–	–	–	1	1
H18	–	–	–	1	1
H19	–	–	2	–	2
H20	–	–	3	–	3
H21	–	–	2	–	2
H22	–	–	2	–	2
H23	–	–	1	–	1
H24	–	–	–	1	1
H25	–	–	–	1	1
H26	–	–	–	1	1

Downloaded from https://academic.oup.com/zoolinnean/article/178/2/410/2674316 by guest on 10 January 2021